Renormalization of the isovector πN amplitude in pionic atoms

E. Friedman and A. Gal
Racah Institute of Physics, The Hebrew University, Jerusalem 91904, Israel

Abstract

The extraction of the isovector s-wave πN amplitude from pionic atoms is studied with special emphasis on uncertainties and their dependence on the *assumptions* made regarding the neutron density distributions in nuclei and on the size of the data base used . Only 'global' analyses of pionic-atom data reveal a discrepancy between the extracted isovector s-wave πN amplitude $b_1 = -0.108 \pm 0.007 \;\; m_\pi^{-1}$ and its free πN counterpart $b_1^{\rm free} = -0.0885^{+0.0010}_{-0.0021} \;\; m_\pi^{-1}$, where the uncertainty in the neutron densities is included in the error analysis. The role of 'deeply bound' pionic atom states is discussed and the reason for failure of these states to provide new information is explained.

PACS: 13.75.-n; 13.75.Gx; 25.80.Hp
Keywords: pionic atoms, s-wave repulsion

Corresponding author: E. Friedman,
Tel: +972 2 658 4667, FAX: +972 2 658 6347,
E mail: elifried@vms.huji.ac.il

April 25, 2003

I. INTRODUCTION

In the past few years there has been renewed interest [1–9] in the extraction of the isovector s-wave πN scattering amplitude near threshold from pionic atom observables. Of particular interest is the relationship between this in-medium amplitude and the corresponding amplitude for the free πN interaction at threshold. This renewed interest in pionic atoms in general, and in the s-wave part of the potential in particular, stems from three recent developments. The first one is the experimental observation of 'deeply bound' pionic atom states in the (d,^{3}He) reaction [7,8,10,11], the existence of which was predicted a decade earlier [12–14]. The second one is the very accurate measurements of the shift and width of the $1s$ level in pionic hydrogen [15] and in pionic deuterium [16,17] which leads to precise values for the s-wave πN scattering lengths (see also Ref. [18]). The third development is the attempt to explain the 'anomalous' s-wave repulsion [19] in terms of a density dependence of the pion decay constant [20], or very recently by constructing the πN amplitude near threshold within a systematic chiral perturbation expansion [21] and in particular imposing on it gauge invariance [22,23].

The so-called anomalous repulsion of the s-wave pionic atom potential is the empirical finding, from fits of optical potentials to pionic atom data, that the strength of the repulsive s-wave potential inside nuclei is typically twice as large as is expected on the basis of the free πN interaction. It is interesting to note that early indications for a very repulsive isovector s-wave amplitude go as far back as 1978 [24] when high precision data became available. Subsequent analyses [25] also indicated such a repulsive amplitude. A key point in this problem are the uncertainties which are associated with the empirical determination of the relevant potential parameters. This problem has been aggravated by recent works in which the 'deeply bound' pionic atom states were granted special status and unfounded implicit assumptions were made on the pion-nucleus optical potential (e.g. Refs. [6,8]). The present work addresses all these issues with the aim of obtaining reliable parameter values for the s-wave part of the pion-nucleus optical potential at threshold, together with realistic estimates of uncertainties. The focus of this work is on the extraction of b_1, the in-medium *isovector* s-wave πN amplitude, from pionic atom data, using the conventional (density-independent) π-nucleus optical potential. It is shown that no definitive conclusions can be reached on whether or not b_1 is renormalized with respect to its free-space value unless the whole bulk of pionic-atom data across the periodic table is used in the analysis. In particular, the deeply bound $1s$ states observed recently in the (d,^{3}He) reaction [7,8] do not offer conclusive evidence for a renormalization of b_1. That applies also to analyses using the deeply bound states together with 'normal' $1s$ states [6].

Section II presents briefly the conventional pion-nucleus potential [26] where the various parameters are defined. Section III is devoted to a discussion of the proton and neutron density distributions which are an essential ingredient of the pion-nucleus optical potential. The proton densities obviously are obtained from the quite well known charge distributions of nuclei but the neutron distributions are generally not known to a sufficient accuracy. For this reason simple but physical parameterizations of the neutron density distributions are introduced, in comparison with available data and with nuclear models. The dependence of the isovector s-wave πN amplitude on the neutron distributions was only marginally touched upon in recent works [4,6] and, therefore, we study in Section IV in some detail the

dependence of this amplitude on both the root mean square (rms) radius of the distribution and, to some extent, on the shape of the distribution. This dependence is translated then into an additional uncertainty of the extracted parameter values. Section IV also presents the results of fits to the data, starting with 'global' fits to 100 and 120 data points and gradually reducing the extent of the data base in order to assess the accuracy of the results, in comparison with other works using 'partial' fits to very limited sets of data [6,8,9] that place special emphasis on the deeply bound $1s$ states in ^{115,119,123}Sn and in ^{205}Pb. The last subsection of Section IV discusses the Seki-Masutani linearization scheme [27] demonstrating the limits of its applicability to pionic-atom studies. In Section V we explain why the deeply bound pionic atom states generally have failed to provide new information on the pion-nucleus interaction. A brief summary and conclusions are presented in Sect. VI.

II. THE PION-NUCLEUS POTENTIAL

The pion-nucleus potential has been extensively discussed (e.g. Ref. [19]), but for completeness a short summary follows.

The interaction of pions at threshold with the nucleus is described by the Klein-Gordon equation of the form:

$$\left[\nabla^2 - 2\mu(B + V_{\rm opt} + V_c) + (V_c + B)^2\right]\psi = 0 \quad (\hbar = c = 1) \tag{1}$$

where μ is the pion-nucleus reduced mass, B is the complex binding energy and V_c is the finite-size Coulomb interaction of the pion with the nucleus, including vacuum-polarization terms. The optical potential $V_{\rm opt}$ used in the present work is of the canonical form due to Ericson and Ericson [26],

$$2\mu V_{\rm opt}(r) = q(r) + \vec{\nabla}\cdot\alpha(r)\vec{\nabla} \tag{2}$$

with

$$\begin{aligned} q(r) = &-4\pi(1+\frac{\mu}{M})\{\bar{b}_0(r)[\rho_n(r)+\rho_p(r)] + b_1[\rho_n(r)-\rho_p(r)]\} \\ &-4\pi(1+\frac{\mu}{2M})4B_0\rho_n(r)\rho_p(r), \end{aligned} \tag{3}$$

$$\alpha(r) = \frac{\alpha_1(r)}{1+\frac{1}{3}\xi\alpha_1(r)} + \alpha_2(r), \tag{4}$$

where

$$\alpha_1(r) = 4\pi(1+\frac{\mu}{M})^{-1}\{c_0[\rho_n(r)+\rho_p(r)] + c_1[\rho_n(r)-\rho_p(r)]\}, \tag{5}$$

$$\alpha_2(r) = 4\pi(1+\frac{\mu}{2M})^{-1}4C_0\rho_n(r)\rho_p(r). \tag{6}$$

In these expressions ρ_n and ρ_p are the neutron and proton density distributions normalized to the number of neutrons N and number of protons Z, respectively, and M is the mass of

the nucleon, $q(r)$ is referred to as the s-wave potential term and $\alpha(r)$ is referred to as the p-wave potential term. The function $\bar{b}_0(r)$ in Eq. (3) is given in terms of the *local* Fermi momentum $k_{\rm F}(r)$ corresponding to the isoscalar nucleon density distribution:

$$\bar{b}_0(r) = b_0 - \frac{3}{2\pi}(b_0^2 + 2b_1^2)k_{\rm F}(r), \tag{7}$$

where b_0 and b_1 are minus the pion-nucleon isoscalar and isovector effective scattering lengths, respectively. The quadratic terms in b_0 and b_1 represent double-scattering modifications of b_0. In particular, the b_1^2 term represents a sizable correction to the nearly vanishing linear b_0 term. Similar modifications of b_1 [21,22] were found by us to be negligibly small. The coefficients c_0 and c_1 in Eq. (5) are the pion-nucleon isoscalar and isovector p-wave scattering volumes, respectively. The parameters B_0 and C_0 in Eqs. (3) and (6) represent s-wave and p-wave absorption, respectively, on pairs of nucleons and as such they have imaginary parts. Dispersive real parts are found to play an important role in pionic atom potentials. The terms with $4\rho_n\rho_p$ were originally written as $(\rho_n + \rho_p)^2$, but the results hardly depend on which form is used. The parameter ξ in Eq. (4) is the usual Ericson-Ericson Lorentz-Lorenz (EELL) coefficient [26]. An additional relatively small term, known as the 'angle-transformation' term (see Eq.(24) of [19]), is also included.

The pion-nucleus optical potential contains nine parameters but only six parameters were varied in the present fits, namely, all the parameters of the s-wave part of the potential and the empirical complex p-wave absorption parameter C_0. The linear p-wave parameters c_0 and c_1 were kept fixed at their respective free πN values, as discussed extensively in Ref. [4]. The EELL coefficient was held fixed at the value $\xi = 1$. It was demonstrated in Ref. [4] that the extracted s-wave parameters are insensitive, with negligibly small variations, to sizable variations of the p-wave parameters, *provided* a fit to the data was made. Note that the extracted parameters b_0 and b_1 are some averages over nuclear densities of in-medium quantities, and if they turn out to be different from the corresponding free πN values then one could refer to a renormalization of the free space values in the nuclear medium.

III. NUCLEAR DENSITY DISTRIBUTIONS

It is evident from the previous section that the nuclear density distributions ρ_p and ρ_n are an essential part of the pion-nucleus potential. Nevertheless, their effect in the present context of studying the s-wave part of the potential and in particular the dependence of the parameter b_1 on the choice of nuclear densities has been hardly addressed, and only briefly so in Refs. [4,6]. This point is studied in more detail in the present work.

Nuclear charge densities are known quite well [28] from studies of elastic scattering of electrons and from finite-size effects in muonic atoms. Density distributions for protons can then be obtained by unfolding the finite size of the charge of the proton. This leads to reliable proton densities, particularly in the surface region, which is the relevant region for producing strong-interaction effects in pionic atoms. The neutron distributions are, however, generally not known to sufficient accuracy. A host of different methods have been applied to the extraction of rms radii of neutron distributions in nuclei [29], including some studies using pionic atoms [25], but the results are sometimes conflicting. Several nuclei have been studied more than others, e.g. isotopes of Ca, Sn and Pb [29–32] but for others there is

no experimental information on neutron densities and one must then rely on calculations based on various models. To complicate things further we note that there is a long history of conflict between values of neutron rms radii derived from experiments using hadronic projectiles and neutron rms radii derived from theoretical calculations. For that reason we have adopted a semi-phenomenological approach that covers a broad range of possible neutron density distributions.

It is shown below that the feature of neutron density distributions which is most effective in determining strong interaction level shifts and widths in pionic atoms is the radial extent, as represented, for example, by r_n, the neutron density rms radius. Other features such as the detailed shape of the distribution have only minor effect. For that reason we chose the rms radius as the prime parameter in the present study. Since r_p, the rms radius for the proton density distribution, is considered to be known, we focus attention on values of the difference $r_n - r_p$. In the analysis of Ref. [4] the nuclear densities were either of the single particle (SP) variety or of the macroscopic type [19] where the values of $r_n - r_p$ were taken from the relativistic mean field (RMF) results of Lalazissis et al. [33] for each of the nuclei involved. Smaller values of $r_n - r_p$ were also used in Ref. [4]. In the present work we vary, among other things, the values of $r_n - r_p$ and we therefore look for a simple parameterization that will be easy to relate to the RMF results. Choosing 43 stable nuclei along the periodic table, the calculated RMF values [33] of $r_n - r_p$ are described very well by the expression

$$r_n - r_p = \alpha \frac{N-Z}{A} + \beta. \tag{8}$$

Figure 1 shows the results of this linear fit in the neutron-proton asymmetry $(N-Z)/A$, where we have arbitrarily assigned an error of ± 0.03 fm to each value of $r_n - r_p$, as a representative value of discrepancies between calculated and experimental charge rms radii. The RMF fit parameters obtained are α=1.51$\pm$0.07 fm, β=$-$0.03$\pm$0.01 fm.

An expression of the form (8) has also been used recently in connection with antiprotonic atoms [34], with parameter values of α=1.01$\pm$0.15 fm, β=$-$0.04$\pm$0.03 fm. Note that antiprotonic atoms are sensitive to nuclear densities well below 10% of the central density and as such it is not very reliable to infer from these data quantities which relate to the bulk of the density. Nevertheless we consider these results as an experimental indication on values of $r_n - r_p$, particularly as they have been used [6] in analyses of pionic atoms. In the present work the neutron rms radii were then varied using Eq.(8) with β=$-$0.035 fm and varying the parameter α between 0.3 and 2.7 fm. This way we have covered a very wide range of possible values of neutron rms radii.

In order to allow for possible differences in the shape of the neutron distribution, the 'skin' and the 'halo' forms of Ref. [34] were used, as well as an average between the two. Assuming a two-parameter Fermi distribution both for the proton (unfolded from the charge distribution) and for the neutron density distributions

$$\rho_{n,p}(r) = \frac{\rho_{0n,0p}}{1+\exp((r-R_{n,p})/a_{n,p})}, \tag{9}$$

then for each value of $r_n - r_p$ in the skin form the same diffuseness parameter for the protons and the neutrons $a_n = a_p$ was used and the R_n parameter was determined from the rms radius r_n. In the halo form the same radius parameter $R_n = R_p$ was assumed and $a_n^{\rm h}$ was

determined from r_n. In the 'average' option the diffuseness parameter was set to be the average of the above two diffuseness parameters $a_n^{\rm ave} = (a_p + a_n^{\rm h})/2$ and the radius parameter R_n was determined from the rms radius r_n. In this way we have used three shapes of the neutron distribution for each value of its rms radius all along the periodic table.

IV. RESULTS AND DISCUSSION

A. Dependence on neutron distribution

For the study of the dependence on the neutron density distribution using the parameterization of Eq. (8) above we first chose a data base of 100 points, from ^{20}Ne to ^{238}U, including the recently published results for the deeply bound $1s$ states in ^{115,119,123}Sn [8] and those for the $1s$ and $2p$ states in ^{205}Pb [7]. Ne was chosen as the lightest element because it is the first element in the periodic table for which the RMF results [33] apply and because we use the two-parameter Fermi parameterization for the densities. Fits to the data were made by varying six of the parameters of the potential, as discussed is Sect. II.

Figure 2 shows χ^2 values for the three types of neutron density, namely, skin, halo and average, as a function of α, the coefficient of the asymmetry parameter $(N-Z)/A$ which determines the value of $r_n - r_p$, see Eq. (8). Also marked by asterisks are the points associated with the particular values of α=1.01 fm and α=1.51 fm, which refer to the '$\bar{p}$' and the RMF prescriptions, respectively. It is easy to conclude from this figure that in the context of global fits to pionic atom data the RMF radii and the skin shape are the favoured option. Note that the minimum of χ^2 implies χ^2/F, the χ^2 per degree of freedom, of 1.8, which represents a very good fit. Increasing the data base to 120 points by adding 20 points from ^{12}C to ^{19}F and repeating the fits, the overall picture remains essentially the same, but the minima become less sharp and imply slightly larger values of χ^2/F. For these additional nuclei (except ^{19}F) a modified harmonic oscillator form [28] was used for the densities.

The above results may be interpreted as indicating that on the average the difference $r_n - r_p$ is described rather well by the RMF model (α=1.5 fm). However, when other experimental data had been analyzed in terms of the difference between rms radii [29–32], quite often smaller values were obtained for $r_n - r_p$, corresponding to α between 1 and 1.5 in Eq. (8). Note that Brueckner-Hartree-Fock calculations generally yield values of $r_n - r_p$ corresponding to $\alpha \sim 1.0$ [35]. We therefore conclude that on the average, rms radii of neutron density distributions are between the values inferred from analyses of antiprotonic atoms (α =1.0) [34] and the predictions of RMF calculations [33].

Turning to the question of the dependence of extracted parameters of the pion-nucleus optical potential on the neutron distribution used in the analysis, Fig. 3 shows the values of b_1 which correspond to the χ^2 results displayed in Fig. 2. It is evident that there is a fairly strong dependence of the extracted b_1 on the prescription chosen for $r_n - r_p$, whereas the dependence on the shape of the density distribution, as indicated by the scatter of points for each value of α, is small. A similar plot of the results of fits to the 120 data points mentioned above is almost indistinguishable from the present figure. Adopting an average value of α= 1.25±0.25 fm as discussed above, one can estimate the additional uncertainty of the extracted potential parameters, due to neutron densities, with the help of plots like the one shown in Fig. 3.

B. Reduced data bases

Several recent publications [6,8] have claimed exceedingly small uncertainties for the parameter b_1 when it is extracted from data bases which are very small in comparison with the 100-120 points of data used above. Such claims are based on adopting several linearizations of terms in the optical potential Eq. (3), notably the Seki-Masutani correlation [27], which are at variance with the results of global fits to large scale data bases, see Refs. [3,5] and the following subsection. We have, therefore, repeated the analysis using progressively reduced data bases in order to examine *in a consistent manner* the dependence of the uncertainties on the data, including also the uncertainty in the neutron density ditribution. The results of this survey are summarized in Tables I and II. The results in Table I are based on the use of the 'RMF skin' neutron densities and the results in Table II are based on the use of the '$\bar{p}$ skin' densities. The 'global 2' and 'global 3' data sets are the ones mentioned in the previous subsection ('global 1' was used in Ref. [4,5]). Three 'partial' data sets are included in the tables, as follows: (i)$1s$ states in light pionic atoms from ^{12}C to ^{28}Si; (ii)$1s$ states in light $N = Z$ pionic atoms plus the deeply bound $1s$ states in ^{115,119,123}Sn [8] and ^{205}Pb [7]; and (iii)only the deeply bound states of (ii). Within each table it is seen that the parameter values are consistent with each other as the size of the data base is changed, but the uncertainties increase as the data base becomes smaller. Note that ReB_0 is different from zero, within errors, only for the global fits. Claims based on 'partial' data sets that no ReB_0 is required to fit the data therefore do not hold for pionic atoms in general. In Tables I and II, for the fit to only deeply bound states, we have set ReB_0=0 since otherwise the convergence proved unreliable with so few data points.

Turning to the role played by the neutron density distributions, it is evident from Tables I and II that the dependence of the extracted parameters on the rms radius of the neutron density distribution must be taken into account in the evaluation of the final results. Table III summarizes the final values of b_1, for α=1.25±0.25 fm (Eq. (8)) as discussed above. Since one deals here with an *average* behaviour of $r_n - r_p$ along the periodic table, the effects of the uncertainty $\Delta\alpha = \pm 0.25$ fm are included in quadrature. Again all the different results for b_1 are consistent with each other, but only those due to global fits to 100-120 data points may be regarded as significantly different from the free πN value [15] of $b_1^{\rm free} = -0.0885^{+0.0010}_{-0.0021}\ m_\pi^{-1}$. Claiming such disagreement by analysing reduced data sets can only be described as unfounded.

C. The Seki-Masutani linearization

Having demonstrated the dependence of the uncertainties of the derived values of b_1 on the size of the data base, we turn now to another problem which has affected recent derivations of this parameter [6–9], namely, the use of the Seki-Masutani (SM) linearization [27]. In the SM scheme the ReB_0 term which is quadratic in the densities is linearized with the help of an 'effective' density such that the two terms with b_0 and ReB_0 are lumped together into a single term $b_0^*\rho(r)$. The existence of correlations between the parameters b_0 and ReB_0 has been known for a long time [27] and it can be seen also in Tables I and II. However, the same tables show also that when large data bases are being used, then the value of each one of these two parameters is reasonably well determined, although not to a very

good accuracy. In order to explicitly show the consequences of using the SM linearization we have repeated the fits reported in Table I with ReB_0 set to zero. The results are summarized in Table IV where it is seen that for the large data bases the values of χ^2 have increased significantly. Note that the 'natural' unit for measuring these increases is χ^2/F, the χ^2 per degree of freedom. For the smaller data sets the increases are not statistically significant, in full agreement with the uncertainties for ReB_0 quoted in Tables I and II. It is concluded that the SM correlation is valid, as may be expected for any non-linear problem over some range of parameters, but when the quality of fit χ^2 criteria are taken into consideration then the use of the SM linearization is unjustified and in the case of large data bases it biases the results.

Another interesting conclusion obtained from Table IV is that when ReB_0 is held fixed the values of b_1 and their uncertainties hardly change compared to the unrestricted analysis. The values of b_0 naturally change in order to compensate for the corresponding changes in ReB_0 but the uncertainties of b_0 go down by almost an order of magnitude, which is unphysical. Since the derivation of b_1 by Geissel et al. [6] is based on "$b_0^* - b_1$ constraints" (b_0^* closely related to our b_0), we conclude that the uncertainties of b_1 obtained in such limited analysis of deeply bound states, which is based on the SM linearization, are bound to be artificially small.

V. THE ROLE OF DEEPLY BOUND STATES

In order to understand the role played by the deeply bound states in pionic atoms of ^{115,119,123}Sn and of ^{205}Pb in global fits, we compare values of χ^2/N, the total χ^2 per point obtained in the fits, with the corresponding values for the contribution of the deeply bound states. For the 'global 2' fit, using RMF-skin densities (Table I), we have χ^2/N=2.0 whereas the contribution of the deeply bound states amounts to 1.0 per point for these states. For the 'global 3' fit the numbers are 1.7 and 0.8, respectively. Removing the deeply bound states from the 'global 2' data and repeating the fit, we find χ^2/N=2.0 and then using the resulting parameters to predict the shifts and widths of the deeply bound states, we get χ^2/N=1.2 for these states. Therefore in all three examples the χ^2/N for the deeply bound states are smaller than the average, signifying that the deeply bound states do not depart from the picture obtained for normal pionic atoms along the periodic table. Limiting the discussion to only 1s states over the periodic table and confronting in Table III the results for light nuclei only with the results for light $N = Z$ nuclei plus the deeply bound states (the latter subset was advocated in Ref. [6]), again it is concluded that the deeply bound states do not provide new information on the isovector s-wave amplitude b_1. This observation is not entirely new and it was shown already in [1] that the deeply bound states in ^{207}Pb were in line with the expectations based on normal pionic atom data. A possible explanation was also indicated in Ref. [1], namely, "the same mechanism which causes the deeply bound states to be narrow also masks the deep interior of nuclei where new effects could possibly be observed".

The fact that the deeply bound pionic atom states have failed to provide new information on the pion-nucleus interaction can be understood from simple arguments of overlap between the atomic wavefunction and the nucleus [5]. Figure 4 displays absolute values squared of the atomic radial wavefunctions multiplied by the nuclear density for a normal 1s state (in ^{20}Ne)

and for a deeply bound $1s$ state (in ^{208}Pb). It is seen that the Coulomb wavefunction would have indeed penetrated deeply into the heavy Pb nucleus, but due to the strong interaction it is repelled such that its overlap with the nucleus is sufficiently small to make the width of the state relatively narrow and thus making the state observable. In fact, the deeply bound $1s$ wavefunction does not overlap with inner regions of the nucleus more so than a normal $1s$ wavefunction does. This shows clearly why deeply bound states do not play any special role in the determination of pionic atom potentials. Expanding the statement made in Ref. [1] we note that the same mechanism which causes the deeply bound states to be narrow and observable, namely, the strong repulsion [12,13] of the wavefunction out of the nucleus, also masks the nuclear interior such that the penetration of the deeply bound pionic atom wavefunction is not dramatically enhanced compared to the normal states.

VI. SUMMARY AND CONCLUSIONS

In this work we have presented a comprehensive analysis of uncertainties for the parameters of the pion-nucleus optical potential which are extracted from experimental strong interaction effects in pionic atoms. Emphasis was placed on the parameter b_1, the isovector s-wave πN amplitude, which has been discussed widely in recent years in connection with possible medium modifications that could also explain the long-standing 'anomalous' repulsion. In addition to errors which are inherent in the χ^2 fit procedure, we have examined errors which are introduced because of the insufficient knowledge of neutron density distributions in nuclei, both in shape and in radial extent. The uncertainties involved in the use of partial data sets were compared with those obtained from global analyses of large amount of data covering all the periodic table. It was shown that only in the latter case the uncertainties are sufficiently small that a discrepancy between the value $b_1 = -0.108 \pm 0.007 \;\; m_\pi^{-1}$ derived from pionic atoms and the corresponding value for the free πN interaction can be established. In particular, the deeply bound states do not provide sufficiently extensive and varied data base in order to constrain b_1 to the required precision. The failure of the deeply bound states to provide meaningful new information on the pion-nucleus interaction has been demonstrated and a simple explanation in terms of overlap arguments was offered.

Finally, we mention Weise's suggestion for a density dependence of b_1 motivated by a partial restoration of chiral symmetry in dense matter [20]. Its application was shown [3,4] to remove most of the anomaly when applied to large data sets. Updating the fit termed 'W' in [4] for the present analysis of the 120 data points and including also the uncertainties due to the neutron densities, we find the following low-density limit values: $b_0 = -0.009 \pm 0.007 \;\; m_\pi^{-1}$ and $b_1 = -0.088 \pm 0.005 \;\; m_\pi^{-1}$, in full agreement with the free πN values [15] of $b_0^{\rm free} = -0.0001^{+0.0009}_{-0.0021} \;\; m_\pi^{-1}$ and $b_1^{\rm free} = -0.0885^{+0.0010}_{-0.0021} \;\; m_\pi^{-1}$. The parameter Re$B_0$ assumes then the value $-0.02 \pm 0.03 \;\; m_\pi^{-4}$, which is most acceptable (see Ref. [3]). Although successful on a phenomenological level, this approach has been deemed controversial. For example, Chanfray et al. [36] have recently discussed the additional medium effect of a σ field on the renormalization of the pion field in dense matter, finding a considerably smaller renormalization effect than that suggested by Weise. On the other hand, Kolomeitsev et al. [22] have argued that Weise's fairly substantial renormalization effect can be derived by considering the energy dependence of $V_{\rm opt}$ within a systematic chiral perturbation expansion and enforcing consistently gauge invariance. This latter suggestion will be addressed in a

forthcoming paper.

We wish to acknowledge the assistance of G. Yaari in the calculation of nuclear densities. This research was partially supported by the Israel Science Foundation.

REFERENCES

[1] E. Friedman and A. Gal, Phys. Lett. B 432 (1998) 235.
[2] P. Kienle and T. Yamazaki, Phys. Lett. B 514 (2001) 1.
[3] E. Friedman, Phys. Lett. B 524 (2002) 87.
[4] E. Friedman, Nucl. Phys. A 710 (2002) 117.
[5] E. Friedman and A. Gal, proceedings of PANIC02, Nucl. Phys. A (in press), nucl-th/0211087.
[6] H. Geissel, H. Gilg, A. Gillitzer, R.S. Hayano, S. Hirenzaki, K. Itahashi, M. Iwasaki, P. Kienle, M. Münch, G, Münzenberg, W. Schott, K. Suzuki, D. Tomono, H. Weick, T. Yamazaki and T. Yoneyama, Phys. Lett. B 549 (2002) 64.
[7] H. Geissel, H. Gilg, A. Gillitzer, R.S. Hayano, S. Hirenzaki, K. Itahashi, M. Iwasaki, P. Kienle, M. Münch, G. Münzenberg, W. Schott, K. Suzuki, D. Tomono, H. Weick, T. Yamazaki and T. Yoneyama, Phys. Rev. Lett. 88 (2002) 122301.
[8] K. Suzuki, M. Fujita, H. Geissel, H. Gilg, A. Gillitzer, R.S. Hayano, S. Hirenzaki, K. Itahashi, M. Iwasaki, P. Kienle, M. Matos, G. Münzenberg, T. Ohtsubo, M. Sato, M. Shindo, T. Suzuki, H. Weick, M. Winkler, T. Yamazaki and T. Yoneyama, nucl-ex/0211023.
[9] T. Yamazaki and S. Hirenzaki, Phys. Lett. B 557 (2003) 20.
[10] T. Yamazaki, R.S. Hayano, K. Itahashi, K. Oyama, A. Gillitzer, H. Gilg, M. Knülle, M. Münch, P. Kienle, W. Schott, H. Geissel, N. Iwasa and G. Münzenberg, Z. Phys. A 355 (1996) 219.
[11] H. Gilg, A. Gillitzer, M. Knülle, M. Münch, W. Schott, P. Kienle, K. Itahashi, K. Oyama, R.S. Hayano, H. Geissel, N. Iwasa, G. Münzenberg and T. Yamazaki, Phys. Rev. C 62 (2000) 025201.
[12] E. Friedman and G. Soff, J. Phys. G: Nucl. Phys. 11 (1985) L37.
[13] H. Toki and T. Yamazaki, Phys. Lett. B 213 (1988) 129.
[14] H. Toki, S. Hirenzaki, T. Yamazaki and R.S. Hayano, Nucl. Phys. A 501 (1989) 653.
[15] H.-Ch. Schröder, A. Badertscher, P.F.A. Goudsmit, M. Janousch, H.J. Leisi, E. Matsinos, D. Sigg, Z.G. Zhao, D. Chatellard, J.-P. Egger, K. Gabathuler, P. Hauser, L.M. Simons and A.J. Rusi El Hassani, Eur. Phys. J. C 21 (2001) 473.
[16] D. Chatellard, J.-P. Egger, E. Jeannet, A. Badertscher, M. Bogdan, P.F.A. Goudsmit, M. Janousch, H.J. Leisi, E. Matsinos, H.-Ch. Schröder, D. Sigg, Z.G. Zhao, E.C. Aschenauer, K. Gabathuler, P. Hauser, L.M. Simons and A.J. Rusi El Hassani, Nucl. Phys. A 625 (1997) 855.
[17] P. Hauser, K. Kirch, L.M. Simons, G. Borchert, D. Gotta, Th. Siems, P. El-Khoury, P. Indelicato, M. Augsburger, D. Chatellard, J.-P. Egger and D.F. Anagnostopoulos, Phys. Rev. C 58 (1998) R1869.
[18] T.E.O. Ericson, B. Loiseau and A.W. Thomas, Phys. Rev. C 66 (2002) 014005.
[19] For a recent review see C.J. Batty, E. Friedman and A. Gal, Phys. Rep. 287 (1997) 385.
[20] W. Weise, Nucl. Phys. A 690 (2001) 98c.
[21] N. Kaiser and W. Weise, Phys. Lett. B 512 (2001) 283.
[22] E.E. Kolomeitsev, N. Kaiser and W. Weise, Phys. Rev. Lett. 90 (2003) 092501.
[23] E.E. Kolomeitsev, N. Kaiser and W. Weise, proceedings of PANIC02, Nucl. Phys. A (in press), nucl-th/0211090.

[24] C.J. Batty, S.F. Biagi, E. Friedman, S.D. Hoath, J.D. Davies, G.J. Pyle and G.T.A. Squier, Phys. Rev. Lett. 40 (1978) 931.
[25] C. García-Recio, J. Nieves and E. Oset, Nucl. Phys. A 547 (1992) 473.
[26] M. Ericson and T.E.O. Ericson, Ann. Phys. [NY] 36 (1966) 323.
[27] R. Seki and K. Masutani, Phys. Rev. C 27 (1983) 2799.
[28] G. Fricke, C. Bernhardt, K. Heilig, L.A. Schaller, L. Schellenberg, E.B. Shera and C.W. De Jager, At. Data Nucl. Data Tables 60 (1995) 177.
[29] C.J. Batty, E. Friedman, H.J. Gils and H. Rebel, Advances in Nuclear Physics 19 (1989) 1.
[30] V.E. Starodubsky and N.M. Hintz, Phys. Rev. C 49 (1994) 2118.
[31] A. Krasznahorkay, M. Fujiwara, P. van Aarle, H. Akimune, I. Daito, H. Fujimura, Y. Fujita, M.N. Harakeh, T. Inomata, J. Jänecke, S. Nakayama, A. Tamii, M. Tanaka, H. Toyokawa, W. Uijen and M. Yosoi, Phys. Rev. Lett. 82 (1999) 3216.
[32] B.C. Clark, L.J. Kerr and S. Hamma, nucl-th/0209052.
[33] G.A. Lalazissis, S. Raman and P. Ring, At. Data Nucl. Data Tables 71 (1999) 1.
[34] A. Trzcińska, J. Jastrzębski, P. Lubiński, F.J. Hartmann, R. Schmidt, T. von Egidy and B. Kłos, Phys. Rev. Lett. 87 (2001) 082501.
[35] K. Pomorski, P. Ring, G.A. Lalazissis, A. Baran, Z. Lojewski, B. Nerlo-Pomorska and M. Warda, Nucl. Phys. A 624 (1997) 349.
[36] G. Chanfray, M. Ericson and M. Oertel, nucl-th/0211035.

TABLES

TABLE I. Parameter values from fits to various sets of pionic atom data based on RMF neutron radii. The linear p-wave parameters were held fixed at c_0=0.22 m_π^{-3}, c_1=0.18 m_π^{-3} and ξ=1.

data	'global 2' ^{12}C to ^{238}U	'global 3' ^{20}Ne to ^{238}U	light $N=Z$ + light $N>Z$ $1s$ only	light $N=Z$ +'deep' $1s$ only	'deep' $1s$ only
points	120	100	22	20	8
χ^2	237	171	54	35	1.6
χ^2/F	2.1	1.8	3.0	2.2	0.3
$b_0(m_\pi^{-1})$	0.000±0.006	−0.001±0.007	−0.009±0.017	−0.016±0.013	−0.007±0.016
$b_1(m_\pi^{-1})$	−0.101±0.003	−0.098±0.003	−0.095±0.013	−0.094±0.007	−0.117±0.030
Re$B_0(m_\pi^{-4})$	−0.085±0.030	−0.082±0.030	−0.048±0.072	−0.017±0.060	0 (fixed)
Im$B_0(m_\pi^{-4})$	0.049±0.002	0.052±0.002	0.049±0.002	0.051±0.002	0.058±0.007
Re$C_0(m_\pi^{-6})$	−0.011±0.008	−0.017±0.009	−0.011 (fixed)	−0.011 (fixed)	−0.011 (fixed)
Im$C_0(m_\pi^{-6})$	0.063±0.003	0.060±0.003	0.063 (fixed)	0.063 (fixed)	0.063 (fixed)

'deep' refers to deeply bound $1s$ states in ^{115,119,123}Sn and ^{205}Pb.

TABLE II. Parameter values from fits to various sets of pionic atom data based on '$\bar{p}$' neutron radii. The linear p-wave parameters were held fixed at c_0=0.22 m_π^{-3}, c_1=0.18 m_π^{-3} and ξ=1.

data	'global 2' ^{12}C to ^{238}U	'global 3' ^{20}Ne to ^{238}U	light $N=Z$ + light $N>Z$ $1s$ only	light $N=Z$ +'deep' $1s$ only	'deep' $1s$ only
points	120	100	22	20	8
χ^2	270	182	65	35	2.1
χ^2/F	2.4	1.9	3.6	2.2	0.4
$b_0(m_\pi^{-1})$	0.009±0.006	0.001±0.007	−0.015±0.017	−0.011±0.015	0.003±0.022
$b_1(m_\pi^{-1})$	−0.114±0.004	−0.109±0.004	−0.103±0.014	−0.114±0.009	−0.143±0.037
Re$B_0(m_\pi^{-4})$	−0.112±0.035	−0.085±0.035	−0.012±0.072	−0.017±0.072	0 (fixed)
Im$B_0(m_\pi^{-4})$	0.049±0.002	0.054±0.003	0.048±0.002	0.051±0.002	0.065±0.008
Re$C_0(m_\pi^{-6})$	−0.010±0.008	−0.010±0.009	−0.010 (fixed)	−0.010 (fixed)	−0.010 (fixed)
Im$C_0(m_\pi^{-6})$	0.063±0.003	0.057±0.004	0.063 (fixed)	0.063 (fixed)	0.063 (fixed)

'deep' refers to deeply bound $1s$ states in ^{115,119,123}Sn and ^{205}Pb.

TABLE III. Average values of b_1 with added uncertainties due to neutron distributions. The free pion-nucleon value [15] is $b_1^{\rm free} = -0.0885^{+0.0010}_{-0.0021}\ m_\pi^{-1}$.

data	'global 2' ^{12}C to ^{238}U	'global 3' ^{20}Ne to ^{238}U	light $N=Z$ + light $N>Z$ $1s$ only	light $N=Z$ +'deep' $1s$ only	'deep' $1s$ only
points	120	100	22	20	8
$b_1(m_\pi^{-1})$	-0.108 ± 0.007	-0.104 ± 0.006	-0.099 ± 0.014	-0.104 ± 0.013	-0.130 ± 0.036

'deep' refers to deeply bound $1s$ states in ^{115,119,123}Sn and ^{205}Pb.

TABLE IV. Same as Table I but with ReB_0=0 (fixed) showing the deterioration in the quality of fits as measured by $\frac{\Delta\chi^2}{\chi^2/{\rm F}}$, the increase of χ^2 in units of χ^2 per degree of freedom.

data	'global 2' ^{12}C to ^{238}U	'global 3' ^{20}Ne to ^{238}U	light $N=Z$ + light $N>Z$ $1s$ only	light $N=Z$ +'deep' $1s$ only
points	120	100	22	20
χ^2	259	190	56	35
χ^2/F	2.3	2.0	2.9	2.1
$\frac{\Delta\chi^2}{\chi^2/{\rm F}}$	9.6	10.6	0.7	0
$b_0(m_\pi^{-1})$	-0.018 ± 0.001	-0.019 ± 0.001	-0.020 ± 0.003	-0.020 ± 0.002
$b_1(m_\pi^{-1})$	-0.102 ± 0.003	-0.099 ± 0.003	-0.093 ± 0.012	-0.094 ± 0.007
Im$B_0(m_\pi^{-4})$	0.048 ± 0.002	0.051 ± 0.002	0.048 ± 0.002	0.050 ± 0.002

'deep' refers to deeply bound $1s$ states in ^{115,119,123}Sn and ^{205}Pb.

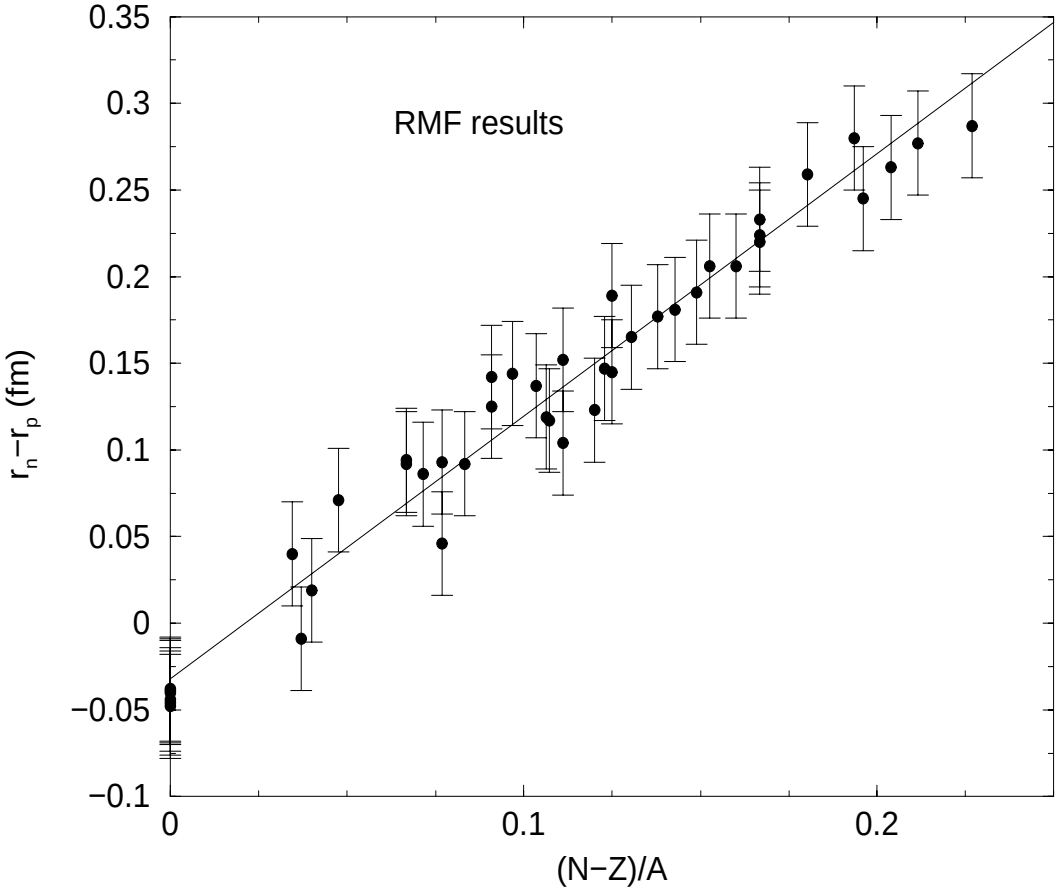

FIG. 1. Fit of a linear expression in the asymmetry parameter to RMF values of $r_n - r_p$.

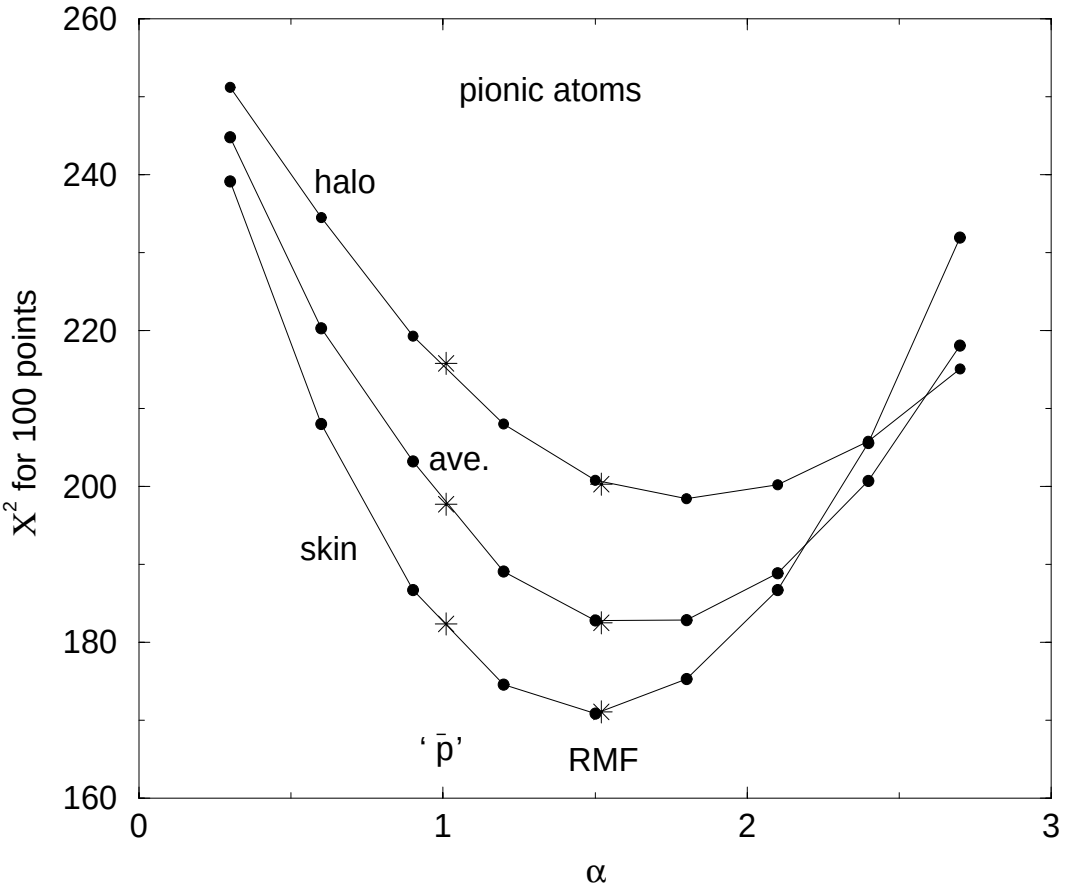

FIG. 2. Values of χ^2 for 100 data points from ^{20}Ne to ^{238}U as function of the slope parameter α in Eq. (8) for three shapes of densities (see text). Points corresponding to '$\bar{p}$' and 'RMF' values for α are marked with asterisks.

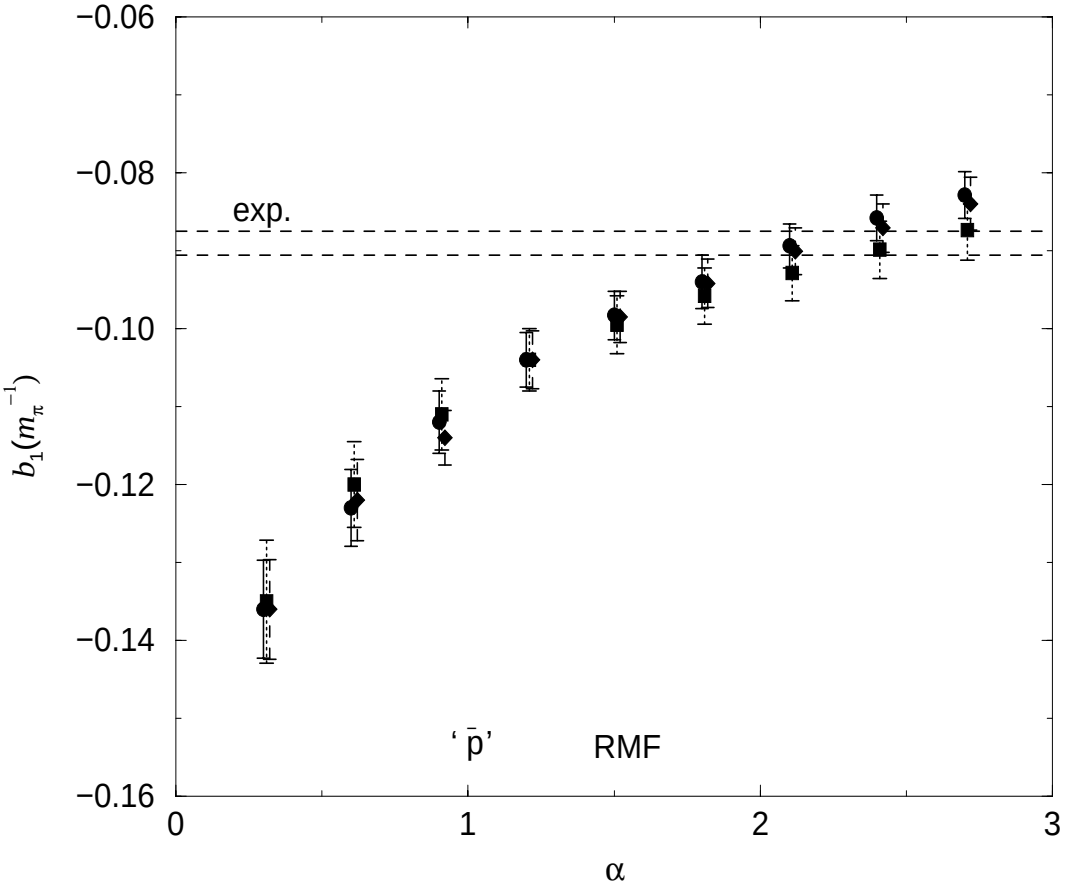

FIG. 3. Values of b_1 from fits to 100 data points from ^{20}Ne to ^{238}U as function of the slope parameter α for three shapes of densities (see Fig. 2). Also shown is the experimental value [15] for $b_1^{\rm free}$.

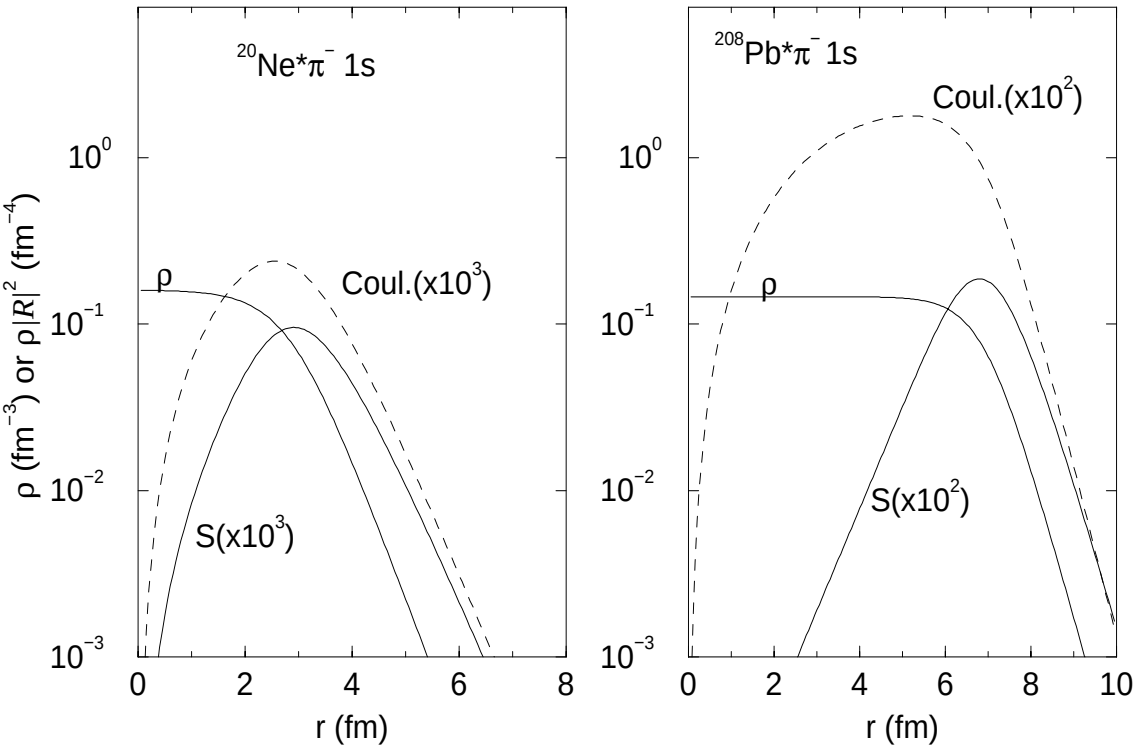

FIG. 4. Nuclear densities and radial densities for pionic 1s states times the nuclear density: dashed for (finite-size) Coulomb potential, solid curves (S) for Coulomb plus strong interaction.